Presentation on:
The Temperature Dependence of 1.3- and 1.5-µm Compressively Strained InGaAs(P) MQW Semiconductor Lasers

Collin Brown

Condensed Matter Journal Club

September 1st, 2016

Lasers in Telecom

- Semiconductor lasers that operate at 1.3 and 1.5 μm are widely used in the telecommunications industry.
- InGaAs(P) lasers have high sensitivity to temperature, and so in commercial applications, additional components are required which add to the cost of the device.
- To fix this problem, the authors propose we first identify the recombination mechanisms and study their temperature dependence.

Recombination Processes

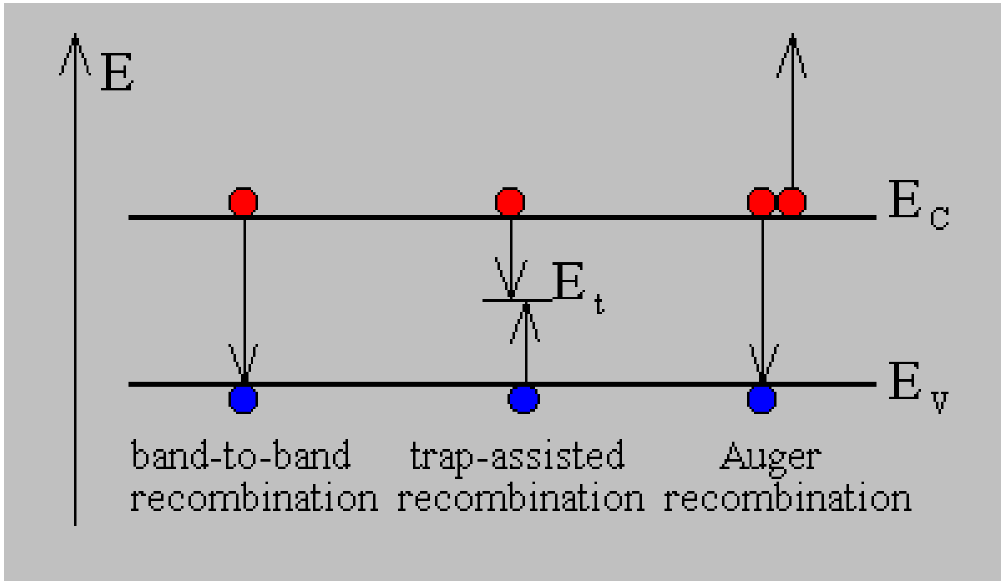

B A C

http://ecee.colorado.edu/~bart/book/recomb.htm

Recombination Processes

$$I = eV(An + Bn^2 + Cn^3) + I_{leak}$$

A – recombination due to traps and defects

B – radiative or bimolecular recombination, associated with spontaneous emission

C – recombination due to Auger processes

I_{leak} – thermal leakage of carriers over the heterobarrier

Dominant Recombination

- If radiative recombination is dominant, then $I \propto n^2$
- If Auger recombination is dominant, then $I \propto n^3$
- So we say that $I \propto n^z$, where z is some value from 2-3
- The total integrated spontaneous emission rate L is related to the injected current.
- Since $L \propto Bn^2$, then $n \propto L^{1/2}$. We can then plug this n into n^z. Then we have $I \propto (L^{1/2})^z$. We take the natural logarithm of both sides.
- $Ln(I) = z\,Ln(L^{1/2})$

Dominant Recombination

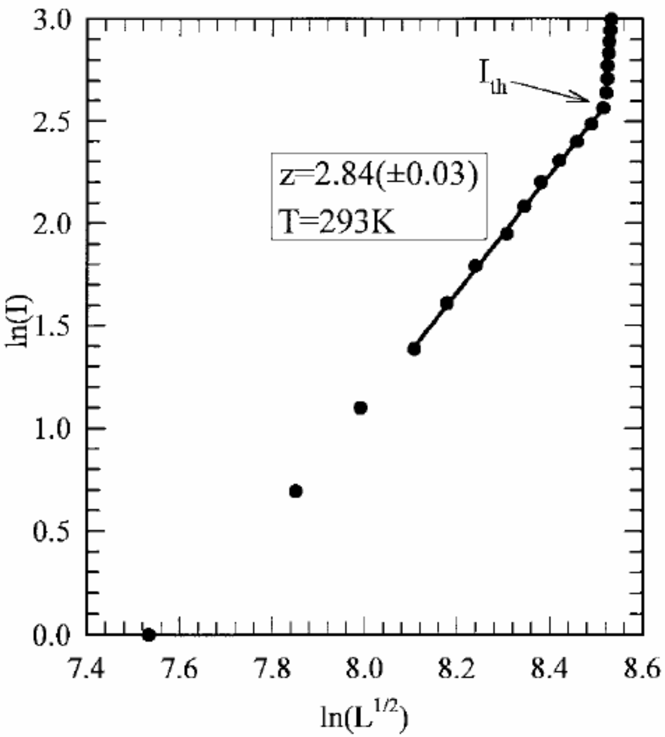

Fig. 3. Graph of $\ln(I)$ versus $\ln(L^{1/2})$ for the 1.5-μm laser at 293 K, showing the method for the determination of z.

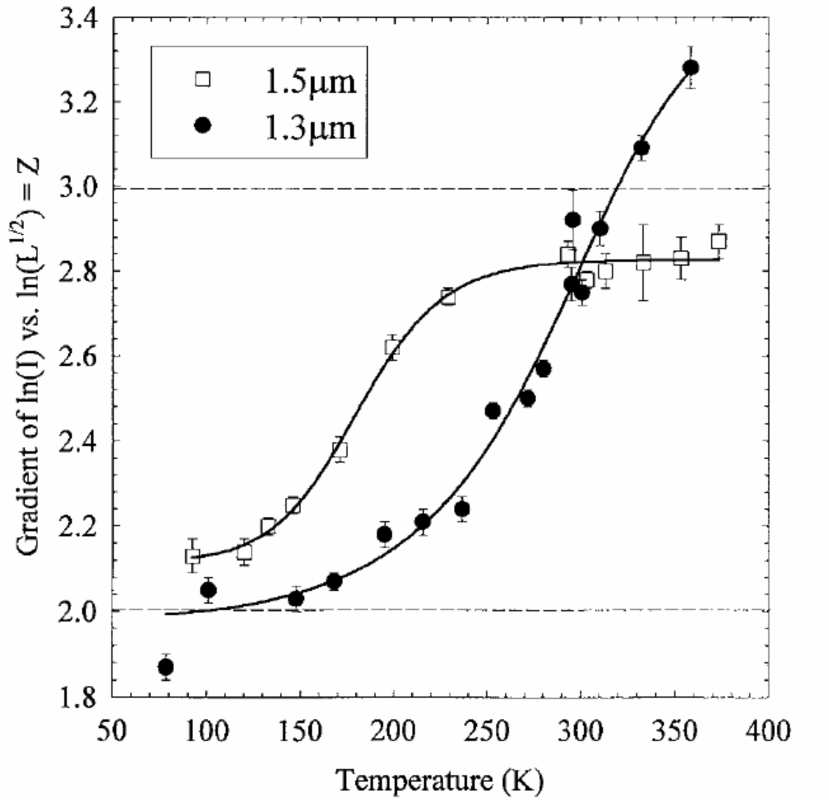

Fig. 4. Variation of z from around 80 K to above 350 K for the 1.5-μm (open squares) and the 1.3-μm (closed circles) lasers.

Threshold Current and Temperature Sensitivity

- $\frac{1}{T_0(I_{TH})} = \frac{1}{I_{TH}} \frac{dI_{TH}}{dT}$
- Using this, we can find temperature sensitivity for radiative threshold current $T_0(I_{Rad})$, where you plug in I_{Rad} for I_{TH}.
- For a QW, the radiative recombination coefficient B changes as $B \propto T^{-1}$
- Threshold carrier density varies as $n_{th} \propto T^{1+x}$
- For the Auger current, the Auger coefficient is assumed to vary as $\mathrm{C} = C_0\, Exp(-E_a/k\,T)$
- We can plug these in to the top equation to get some temperature dependence

Threshold Current and Temperature Sensitivity

- Radiative Current - $T_0(I_{Rad}) = \frac{T}{1+2x}$

- Auger Current - $T_0\left(I_{Aug}\right) = \frac{T}{3 + 3x + E_a/(k\ T)}$

- The x is introduced to account for nonidealities in the laser

Experiment

- Pure spontaneous emission is collected from the side of the lasers via an optical fiber.
- This light is then sent to an optical spectrum analyzer (OSA)

Effect of Bandgap on Auger processes

- Here a pressure vessel is used to subject the sample to high pressures. The application of pressure increases the bandgap E_g at the Brillouin zone center.
- "In an ideal QW, the radiative current increase is approximately equal to ${E_g}^2$, while the Auger recombination rate decreases with increasing bandgap."

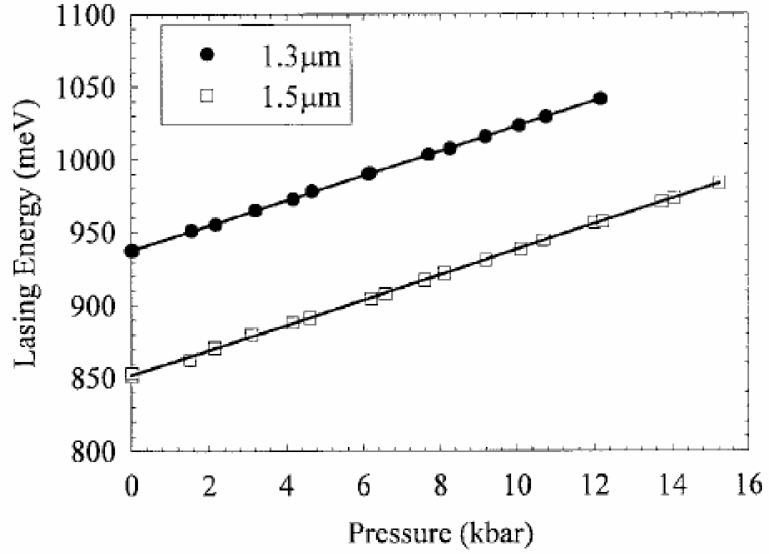

Fig. 5. Graph showing the variation of lasing energy with pressure for the 1.3-μm laser (closed circles) and the 1.5-μm laser (open squares).

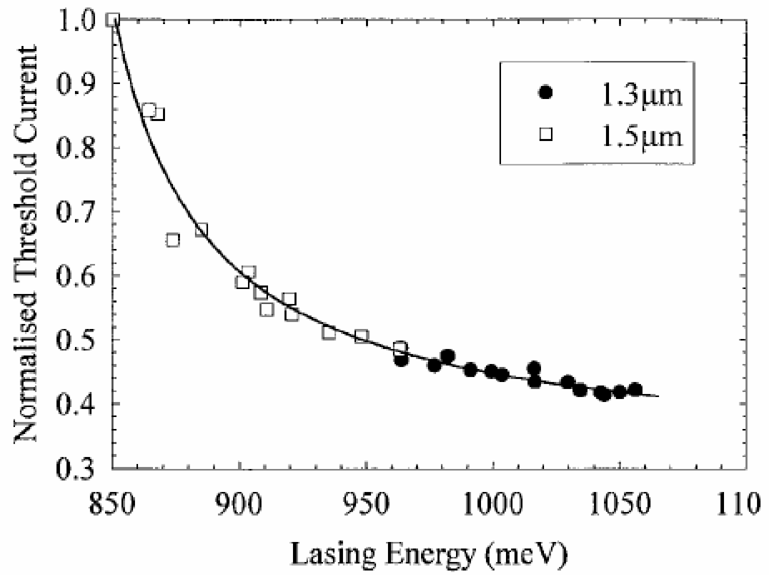

Fig. 6. Normalized threshold current as a function of lasing energy. The 1.3-μm data were normalized to the value of the 1.5-μm data at the point where the 1.5-μm device lased at 1.3 μm.

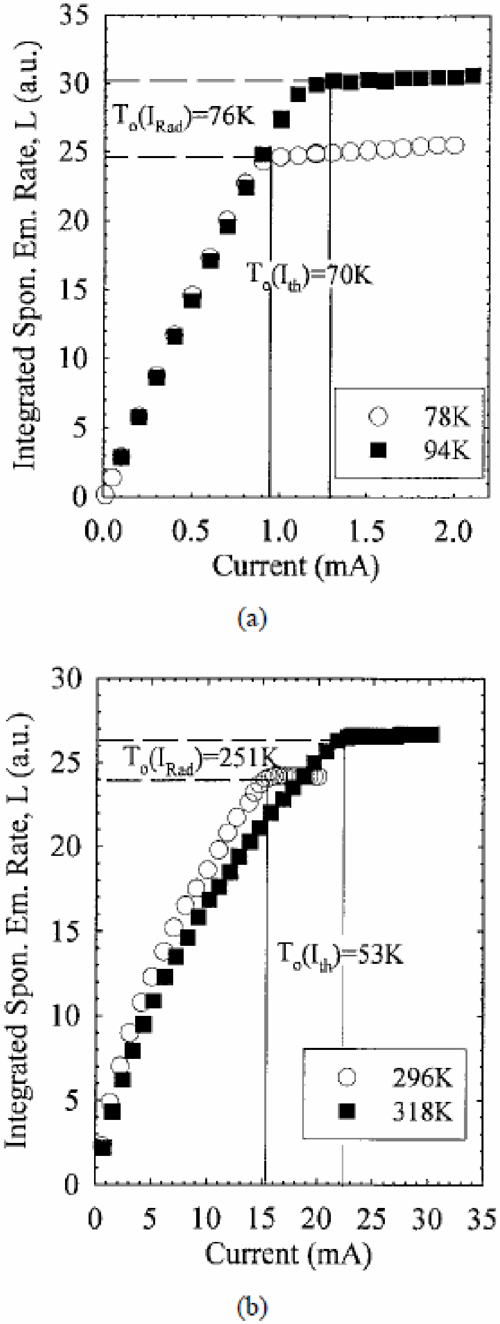

Fig. 7. Integrated spontaneous emission rate as a function of current for the 1.5-μm laser at temperatures around (a) 86 K and (b) 307 K.

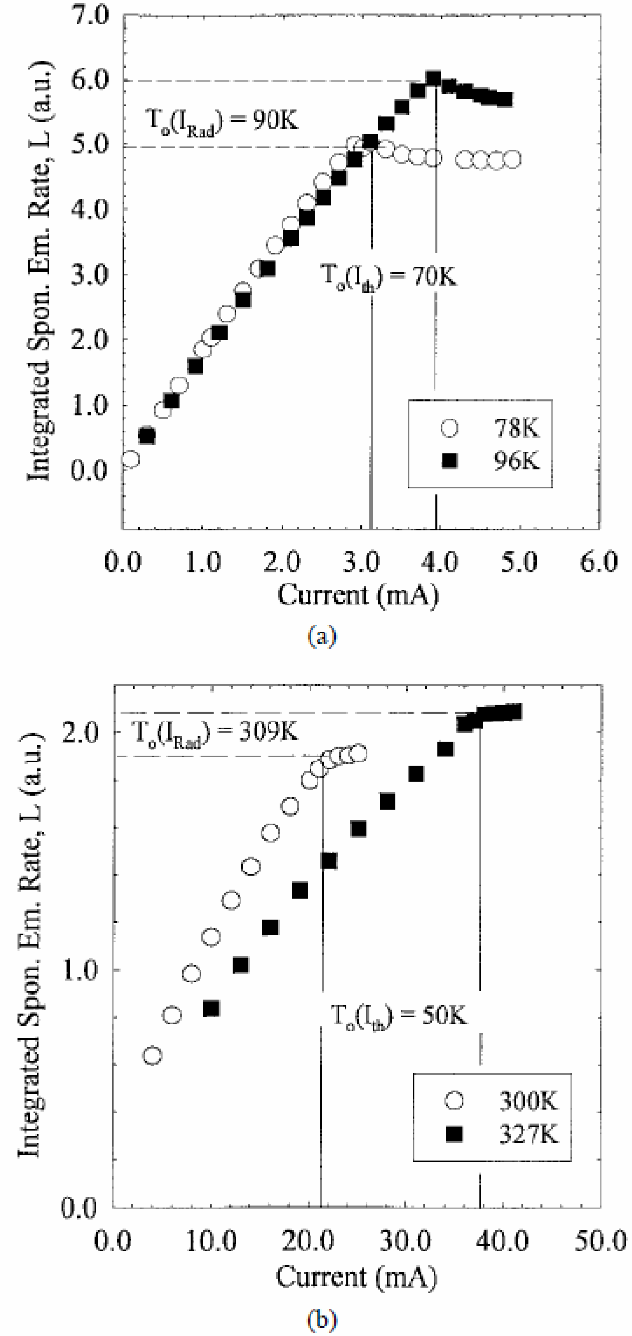

Fig. 8. Integrated spontaneous emission rate as a function of current for the 1.3-μm laser at temperatures around (a) 87 K and (b) 314 K.

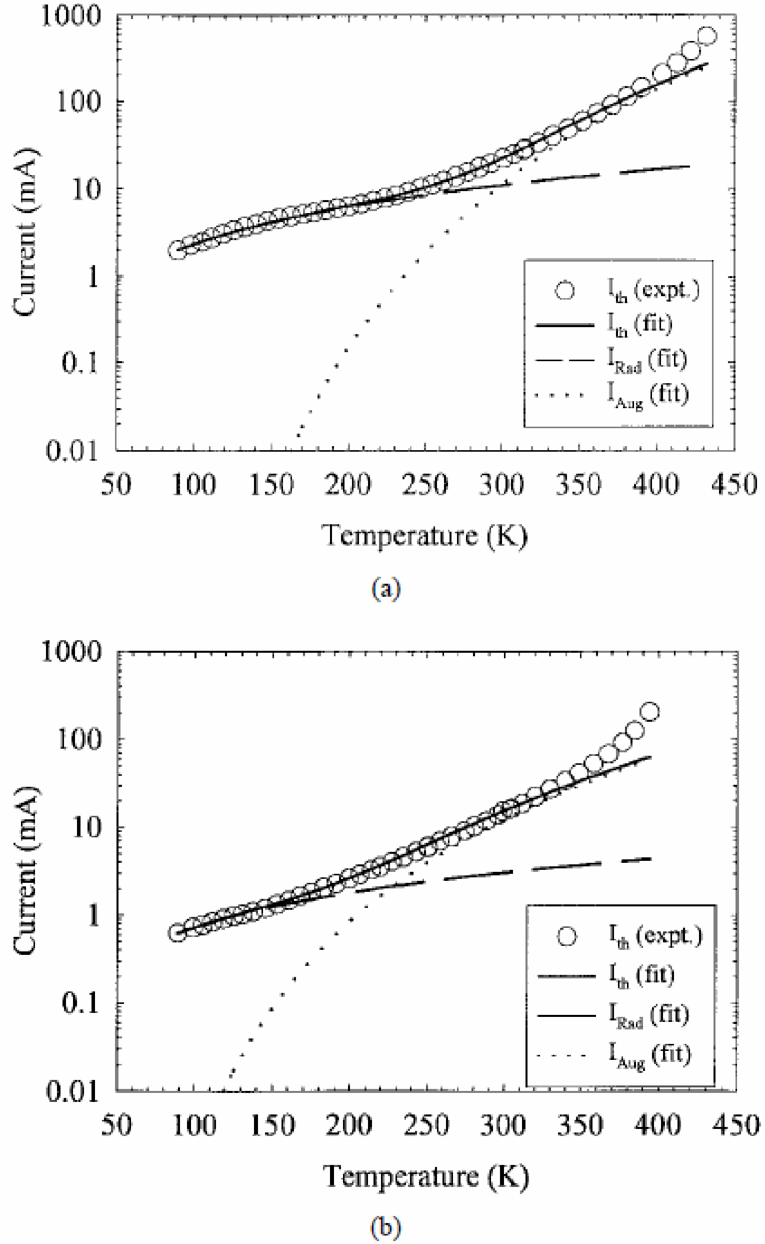

Fig. 9. Threshold current on a log scale as a function of temperature for (a) the 1.3-μm laser and (b) the 1.5-μm laser (open circles). The solid, dashed, and dotted lines are the fitted variations of the threshold current, radiative current, and Auger current, respectively.

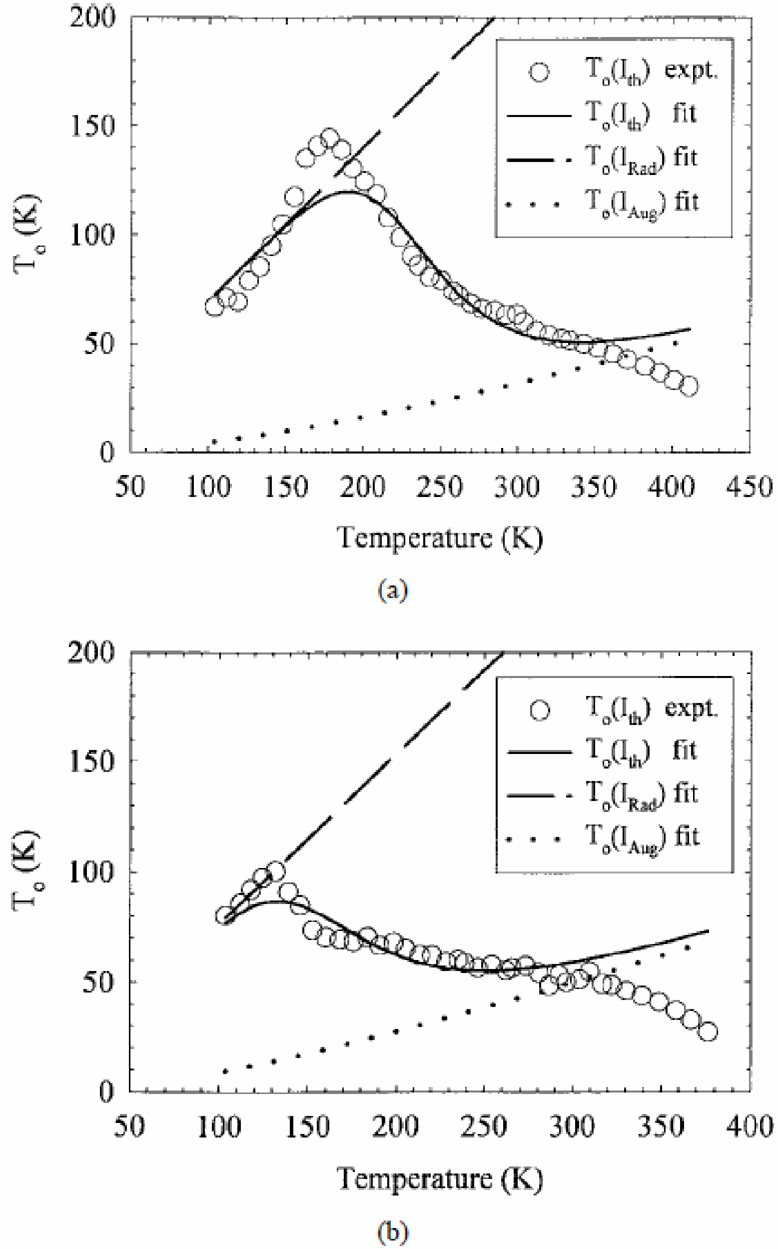

Fig. 10. Characteristic temperature for the threshold current $T_o(I_{th})$ (open circles) as a function of temperature for (a) the 1.3-μm laser and (b)-1.5 μm laser. The solid, dashed, and dotted lines are the fitted T_o values for the threshold current, radiative current, and Auger current, respectively.

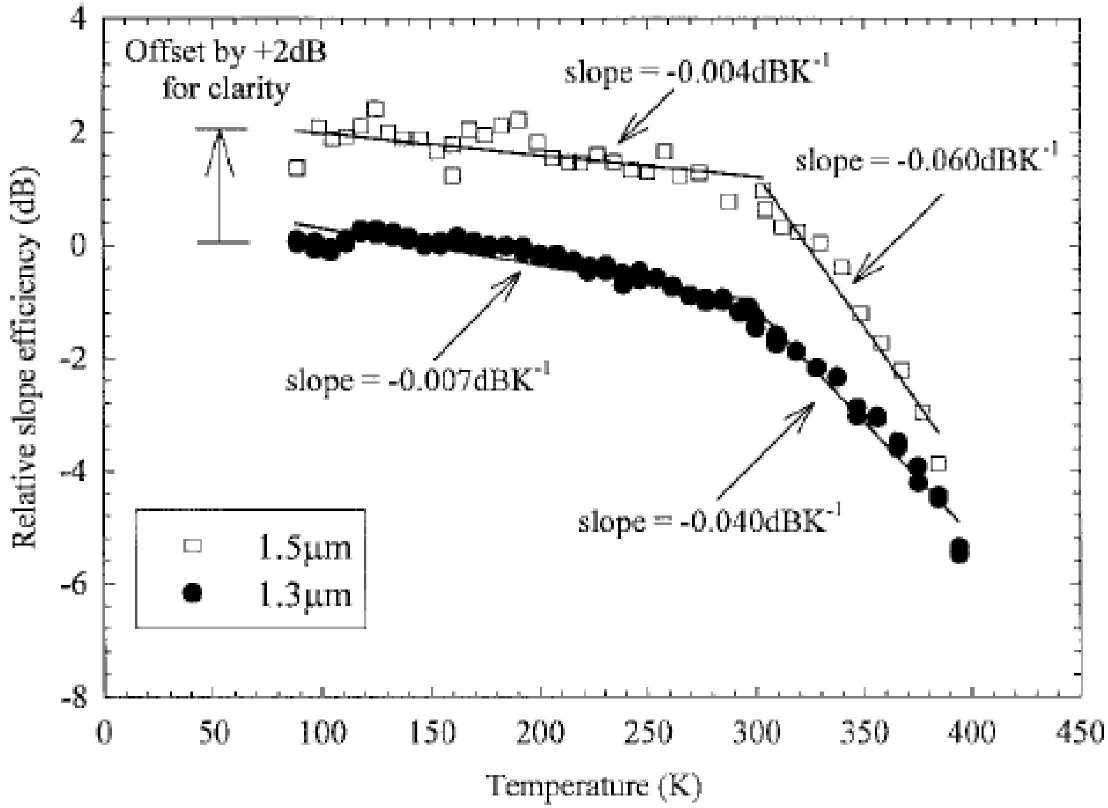

Fig. 11. Relative slope efficiency as a function of temperature for 1.3-μm lasers (closed circles) and 1.5-μm lasers (open squares). The data are offset for clarity. A rapid decrease of η_d above room temperature can be seen.

$$\frac{1}{\eta_d} = \frac{1}{\eta_i}\left(1 + \frac{\alpha_i L_{cav}}{\ln(\frac{1}{R})}\right)$$

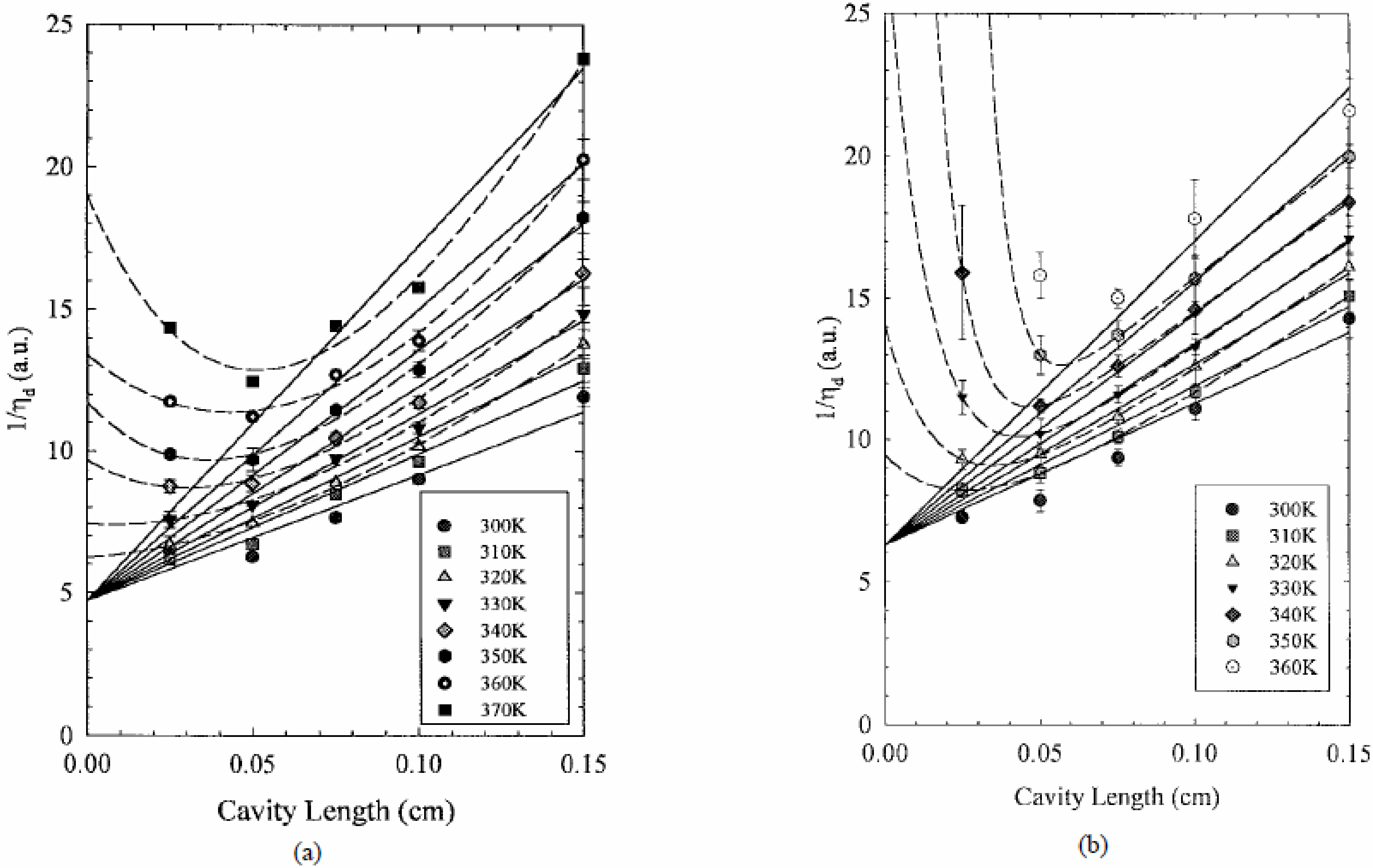

Fig. 12. The inverse of the differential quantum efficiency as a function of cavity length and temperature for (a) 1.3-μm lasers and (b) 1.5-μm lasers. The solid lines are least-squares fits to the data from the four longest cavity lengths for a common intercept. The dashed lines show how dramatically $1/\eta_d$ increases for the shorter cavity length lasers.

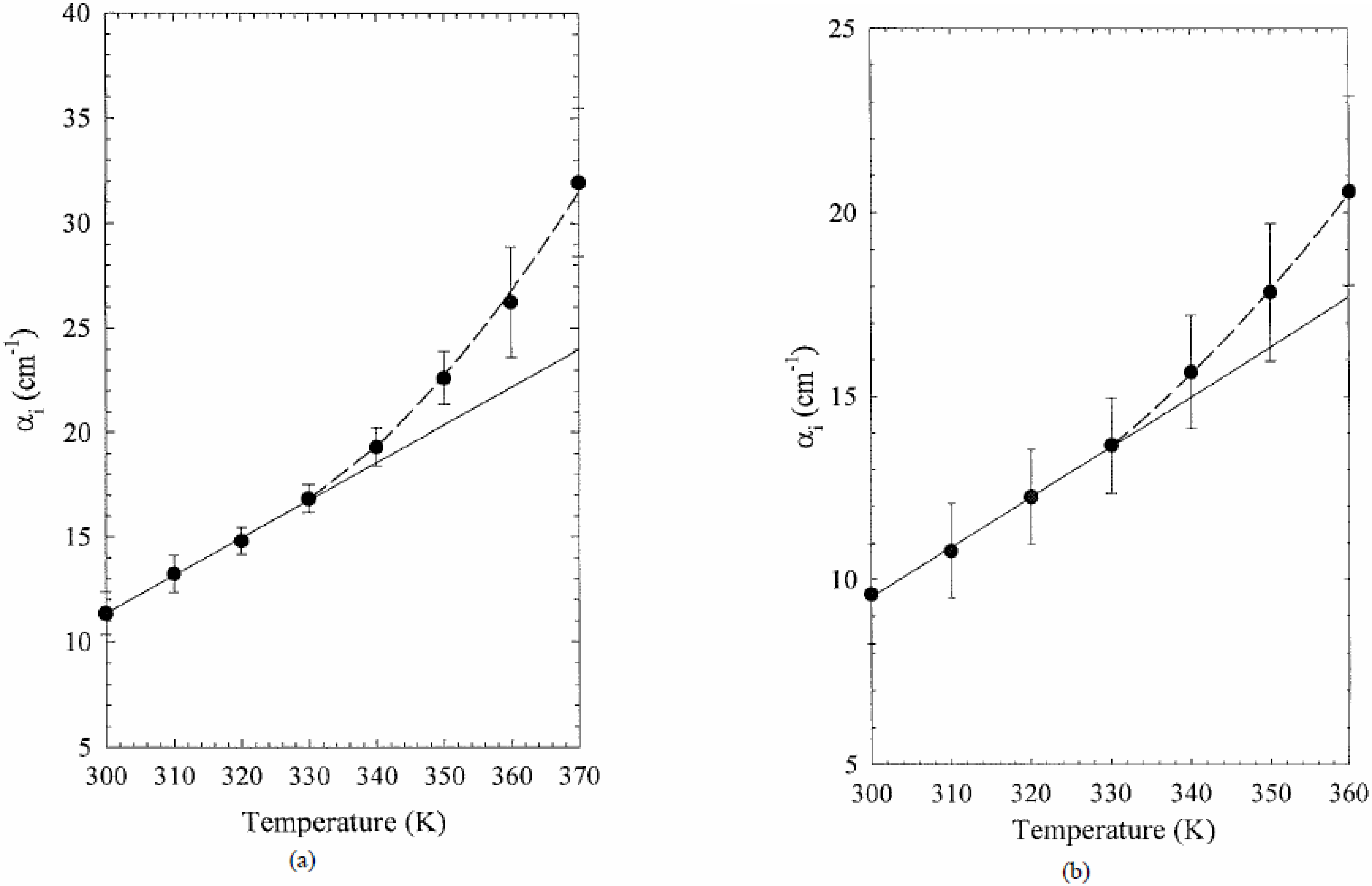

Fig. 13. Internal loss α_i as a function of temperature for (a) 1.3-μm eight-QW InGaAsP lasers and (b) 1.5-μm 4-QW InGaAs lasers. A superlinear increase of α_i above ~330 K can clearly be seen.

Conclusion

- At low temperature, the threshold current and its temperature sensitivity are governed by radiative recombination.
- Past a certain breakpoint, and at room temperature, Auger recombination becomes a factor.
- At room temperature, the strong contribution of Auger recombination results in $I \propto n^3$
- Above room temperature, the increase in threshold current may come from increased optical losses and carrier overflow into the barrier and SCH regions.